Taylor & Francis
Taylor & Francis Group

Journal of Toxicology and Environmental Health, Part A

ISSN: 1528-7394 (Print) 1087-2620 (Online) Journal homepage: http://www.tandfonline.com/loi/uteh20

Titanium Dioxide (TiO_2) Nanoparticles Induce JB6 Cell Apoptosis Through Activation of the Caspase-8/Bid and Mitochondrial Pathways

Jinshun Zhao , Linda Bowman , Xingdong Zhang , Val Vallyathan , Shih-Houng Young , Vincent Castranova & Min Ding

To cite this article: Jinshun Zhao , Linda Bowman , Xingdong Zhang , Val Vallyathan , Shih-Houng Young , Vincent Castranova & Min Ding (2009) Titanium Dioxide (TiO_2) Nanoparticles Induce JB6 Cell Apoptosis Through Activation of the Caspase-8/Bid and Mitochondrial Pathways, Journal of Toxicology and Environmental Health, Part A, 72:19, 1141-1149, DOI: 10.1080/15287390903091764

To link to this article: https://doi.org/10.1080/15287390903091764

Journal of Toxicology and Environmental Health, Part A, 72: 1141–1149, 2009

ISSN: 1528-7394 print / 1087-2620 online
DOI: 10.1080/15287390903091764

Taylor & Francis
Taylor & Francis Group

Titanium Dioxide (TiO_2) Nanoparticles Induce JB6 Cell Apoptosis Through Activation of the Caspase-8/Bid and Mitochondrial Pathways

Jinshun Zhao, Linda Bowman, Xingdong Zhang, Val Vallyathan, Shih-Houng Young, Vincent Castranova, and Min Ding

Pathology and Physiology Research Branch, Health Effects Laboratory Division, National Institute for Occupational Safety and Health, Morgantown, West Virginia, USA

Titanium dioxide (TiO_2), a commercially important material, is used in a wide variety of products. Although TiO_2 is generally regarded as nontoxic, the cytotoxicity, pathogenicity, and carcinogenicity of TiO_2 nanoparticles have been recently recognized. The present study investigated TiO_2 nanoparticle-induced cell apoptosis and molecular mechanisms involved in this process in a mouse epidermal (JB6) cell line. Using the 3-(4,5-dimethylthiazolyl-2)-2, 5-diphenyltetrazolium bromide (MTT) assay, TiO_2 nanoparticles were found to exhibit higher cytotoxicity than fine particles. YO-PRO-1 iodide (YP) staining demonstrated that both TiO_2 nanoparticles and fine particles induced cell death through apoptosis. The signaling pathways involved in TiO_2 particle-induced apoptosis were investigated. Western-blot analysis showed an activation of caspase-8, Bid, BAX, and caspase-3 and a decrease of Bcl-2 in JB6 cells treated with TiO_2 particles. Time-dependent poly(ADP)ribose polymerase (PARP) cleavage induced by TiO_2 nanoparticles was observed. TiO_2 particles also induced cytochrome *c* release from mitochondria to cytosol. Further studies demonstrated that TiO_2 nanoparticles induced significant changes in mitochondrial membrane permeability, suggesting the involvement of mitochondria in the apoptotic process. In conclusion, evidence indicated that TiO_2 nanoparticles exhibit higher cytotoxicity and apoptotic induction compared to fine particles in JB6 cells. Caspase-8/Bid and mitochondrial signaling may play a major role in TiO_2 nanoparticle-induced apoptosis involving the intrinsic mitochondrial pathway. Unraveling the complex mechanisms associated with these events may provide further insights into TiO_2 nanoparticle-induced pathogenicity and potential to induce carcinogenicity.

Nanomaterials are newly developed products and are currently of interest in a variety of applications such as electronics, reinforced rods, micro-fabricating, cosmetics, and biosensors. The number of workers producing or using nanomaterials is expected to grow accordingly. While benefits of nanotechnology are widely publicized, concerns about the environment and occupational health risks are increasing (Luther, 2004; Tabet et al., 2009).

TiO_2 is a poorly soluble particulate that has been widely used as a white pigment in the production of paints, paper, plastics, welding rod-coating material, and food colorant. Nano-sized or ultrafine TiO_2 (<100 nm) is used increasingly in other industrial products, such as toothpastes, sunscreens, cosmetics, pharmaceuticals, and food products (Kaida et al., 2004; Wang et al., 2007; Wolf et al., 2003). Human exposure may occur during both manufacturing and use. Such widespread use and its potential entry in the body through dermal, ingestion, and inhalation routes suggest that TiO_2 nanoparticles pose a potential exposure risk to humans, livestock, and the ecosystem (Long et al., 2007). TiO_2 particles have been used traditionally for many years as a "negative control" in many *in vitro* and *in vivo* dust-induced toxicological investigations. However, this view was challenged when lung tumors were found in rats after lifetime exposure to high concentrations of pigment grade TiO_2 (Lee et al., 1985). Furthermore, the International Agency for Research on Cancer (IARC) recently classified TiO_2 as a Group 2B carcinogen based on mechanistic and animal studies (IARC, 2006). In addition to the potential inhalation health effects, one study reported that TiO_2 nanoparticles in sunscreen formulations penetrate the human stratum corneum (Lademann et al., 1999). Thus, epidermal cells would come into contact with TiO_2 nanoparticles to potentially produce

Received 6 February 2009; accepted 16 March 2009.

The findings and conclusions in this report are those of the authors and do not necessarily represent the views of the National Institute for Occupational Safety and Health. We thank Dr. Shengqiao Li for statistical analysis, Diane Schwegler-Berry and Sherri Friend for image analysis, and Donna Pack for surface area analysis.

Address correspondence to Min Ding, MD, PhD, Pathology and Physiology Research Branch, Health Effects Laboratory Division, National Institute for Occupational Safety and Health, 1095 Willowdale Road, Morgantown, WV 26505, USA. E-mail: mid5@cdc.gov

epidermal interactions and toxicity. There is strong evidence to suggest that the pathogenic effects of TiO_2 depend on particle size (Churg et al., 1999). Another report demonstrated that TiO_2 nanoparticles induced impairment of macrophage function, persistent high frequency of inflammatory reactions, and increased pulmonary retention compared to TiO_2 fine particles (Baggs et al., 1997). TiO_2 nanoparticles also enter the epithelium more rapidly and are translocated in greater proportion to the subepithelial space compared to fine particles (Churg et al., 1998). Moreover, recent studies demonstrated that TiO_2 nanoparticles damage brain microglia cells and induce Syrian hamster embryo (SHE) cell apoptosis (Long et al., 2007; Rahman et al., 2002). However, the molecular mechanisms involved in the process of apoptosis induced by TiO_2 nanoparticles have not been clearly elucidated.

Apoptosis is a highly regulated process that is involved in normal physiological as well as pathological conditions (Raff, 1992; Steller, 1995; White et al., 2001; Wyllie et al., 1980). There is extensive and growing interest in the role of apoptosis and apoptotic signals in inflammatory and immune cells. Inhibition of apoptosis by gene deletion strategies or by caspase inhibitors abrogates the pathologic effects of inflammatory agents (Bardales et al., 1996), supporting the potential role of apoptosis in inflammatory and immunopathologic disorders. Some diseases may be produced by a malfunction of the apoptotic mechanism. An inefficient elimination of mutated cells may favor carcinogenesis, but failure to clear inflammatory cells may prolong the inflammation because of the release of damaging histotoxins (Lombaert et al., 2004). However, excessive apoptosis was shown to contribute to pulmonary fibrosis in mice and hepatic failure in rats (Durmowicz & Stenmark, 1999; Kuwano et al., 1999). Furthermore, enhanced apoptosis may indirectly trigger compensatory cell proliferation to ensure tissue homeostasis and promote the fixation of mutagenic events and/or multiplication of mutated cells. Evidence indicates that apoptosis is also involved in certain pulmonary disorders, such as acute lung injury, diffuse alveolar damage, idiopathic pulmonary fibrosis, and other lung disorders produced by bleomycin, silica or endotoxin, and deposition of immune complexes (Bardales et al., 1996; Kuwano et al., 1999; Levine, 1997; Matute-Bello et al., 2001). Therefore, the apoptotic properties may be important in the mechanisms underlying pathogenicity induced by TiO_2 nanoparticles.

Therefore, the objective of the present study was to (1) compare cytotoxicity and apoptosis induced by TiO_2 nanoparticles and fine particles, and (2) characterize the major apoptotic pathways induced by TiO_2 nanoparticles. These studies should provide insight into the role of apoptosis in the pathogenicity and carcinogenicity induced by TiO_2 nanoparticles.

MATERIALS AND METHODS

Materials

TiO_2 nanoparticles (commercial grade, Aeroxide TiO_2 P-25, primary size 21 nm, 80/20 anatase/rutile) were obtained from Degussa Corp. (Parsippany, NJ). TiO_2 fine particles (titanium(IV) oxide, rutile, <5 μm) were purchased from Sigma-Aldrich (St. Louis, MO). Eagle's minimum essential medium (EMEM) was obtained from Whittaker Biosciences (Walkersville, MD). Fetal bovine serum (FBS), trypsin, pencillin/streptomycin, and L-glutamine were purchased from Life Technologies, Inc. (Gaithersburg, MD). YO-PRO-1 iodide (YP) and propidium iodide (PI) were purchased from Molecular Probes (Eugene, OR). Anti-h/m caspase-8 antibody was obtained from R&D Systems (Minneapolis, MN). Total AKT, Bid, and cleaved caspase-3 antibodies were purchased from Cell Signaling Technology (Beverly, MA). All other antibodies were obtained from Santa Cruz Biotechnology Co. (Santa Cruz, CA). The cell proliferation kit I was obtained from Roche Applied Science (Penzberg, Germany). The mitochondria staining kit was purchased from Sigma-Aldrich.

Preparation of TiO_2 Nanoparticles and Fine Particles

Stock solutions of TiO_2 nanoparticles or fine particles were prepared in sterile phosphate-buffered saline (PBS, 10 mg/ml) by sonication for 30 s using a Branson sonifier 450 (Branson Ultrasonics Corp., Danbury, CT). Particle suspensions then were kept on ice for 15 s and sonicated again on ice for a total of 3 min at a power of 400 W. Before use, TiO_2 nanoparticles or fine particles were diluted to desired concentrations in fresh culture medium. All samples were prepared under sterile conditions.

Surface Area and Size Distribution Measurement

Surface area of TiO_2 particles was measured using the Gemini 2360 surface area analyzer (Micromeritics, Norcross, GA) by the gas absorption technique according to the manufacturer's instructions. The size distribution of TiO_2 particles was detected using scanning electron microscopy. Briefly, TiO_2 particles were prepared by sonication. Then the samples were diluted in double-distilled water and air-dried onto a carbon planchet. Images were collected on a scanning electron microscope (Hitachi S-4800; Japan) according to the manufacturer's instructions. Optimas 6.5 image analysis software (Media Cybernetics, Bethesda, MD) was used to measure the diameter of TiO_2 particles.

Cell Culture

Mouse epidermal JB6 cells were maintained in 5% FBS EMEM containing 2 m*M* L-glutamine and 1% penicillin–streptomycin (10,000 U/ml penicillin and 10 mg/ml streptomycin) at standard culture conditions (37°C, 80% humidified air, and 5% CO_2). For all treatments, cells were grown to 80% confluence.

Cytotoxicity Measurements

Cytotoxicity of TiO_2 nanoparticles or fine particles on JB6 cells was assessed by an MTT assay kit following the

manufacturer's instructions. Briefly, cells were plated at a density of 10^4 cells/well in a 96-well plate. The cells were grown for 24 h and treated with various concentrations of TiO_2 particles. After 24 h of incubation, 10 (μl MTT labeling reagent was added in each well and the plates were further incubated for 4 h. Afterward, 100 (μl solubilization solution was added to each well, and the plate was incubated overnight at 37°C. The optical density (OD) of the wells was measured at a wavelength of 575 nm with reference of 690 nm using an enzyme-linked immunosorbent assay (ELISA) plate reader. Results were calibrated with OD measured without cells in culture.

Apoptosis Detection

Apoptosis induced by TiO_2 particles in cells was determined by YP staining. Briefly, JB6 cells were seeded onto a 24-well plate overnight. Then cells were treated with/without various concentrations of TiO_2 nanoparticles or fine particles for 24 h. Before microscopy, YP was added into the cultures at a final concentration of 10 μg/ml for 1 h. Cells were washed two times with EMEM medium. Apoptotic cells were monitored using a fluorescence microscope (Axiovert 100M). YP stains the nucleus green if the cell is apoptotic. The percentage of cells exhibiting apoptosis was counted and calculated.

Distinguishing Between Apoptosis and Necrosis

Dual staining using YP and PI was used to distinguish between apoptosis or necrosis as previously described (Boffa et al., 2005; Debby Gawlitta et al., 2004) with some modifications. JB6 cells were seeded onto 24-well plates and incubated overnight. Then, cells were treated with/without various concentrations of TiO_2 nanoparticles. One hour later, YP and PI were added into the cultures at a final concentration of 10 μg/ml and 1 μ*M*, respectively. The progression of cell death in the living cultures was monitored at different time points using a fluorescence microscope (Axiovert 100M). YP-stained cells (apoptotic cells) were detected with a blue excitation filter. PI-stained cells (necrotic cells) were measured with a green excitation filter.

Western Blot Analysis

Briefly, JB6 cells were plated onto a six-well plate. The cultures were grown for 24 h and then starved in 0.1% FBS EMEM overnight. Cells were treated with/without TiO_2 nanoparticles or fine particles. After treatment, the cells were extracted with 1 × sodium dodecyl sulfate (SDS) sample buffer supplied with protease inhibitors. Protein concentration was determined using the bicinchoninic acid method (Pierce, Rockford, IL). Equal amounts of proteins were separated by 12.5% sodium dodecyl sulfate polyacrylamide gel electrophoresis (SDS-PAGE) gels and transferred to polyvinylidene fluoride (PVDF) membrane (Invitrogen, Carlsbad, CA). Immunoblots for expression of caspase-8, Bid, Bcl-2, BAX, caspase-3, PARP, and cytochrome *c* were carried out as described in the protocol from New England Biolabs (Ipswich, MA). Experiments were performed three or more times, and equal loading of protein was ensured by measuring total Akt or alpha-tubulin expression.

To prepare the subcellular fractionation, cells were washed twice with cold PBS. Then, cells were lysed in 100 μl of cold isolation buffer A (20 m*M* HEPES/10 m*M* KCl/1.5 m*M* $MgCl_2$/1 m*M* ethylenediamine tetraacetic acid [EDTA]/1 m*M* EGTA/1 m*M* dithiothreitol [DTT]) supplemented with protease inhibitor cocktail and 250 m*M* sucrose. After incubating on ice for 15 min, the cells were broken by passing through 22-gauge needles 25 times. The lysate was centrifuged at 800 × g for 5 min to remove unbroken cells and nuclei. The supernatant was then recentrifuged (10,000 × g, 30 min, 4°C) to obtain a pellet. The resultant supernatant was the cytosolic fraction and the pellet contained mitochondria. The cytosolic fraction was diluted using 100 μl of 2 × SDS sample buffer. The mitochondrial pellet was resuspended in 1× SDS sample buffer.

Detection of Changes of Mitochondrial Membrane Permeability

JB6 cells were seeded onto a 24-well plate overnight. Cells were treated with/without TiO_2 nanoparticles for 24 h. Changes of mitochondrial membrane permeability were evaluated using the mitochondrial staining kit. Briefly, a staining mixture was prepared by mixing the staining solution with an equal volume of the EMEM medium. Cells were incubated in the staining mixture (0.4 ml/well) for 30 min at 37°C in a humidified atmosphere containing 5% CO_2. Thereafter, cells were washed in the medium two times, followed by addition of fresh medium. Mitochondrial membrane permeability was monitored using a fluorescence microscope (Axiovert 100M).

Statistical Analysis

Data are presented as means ± standard errors (SE) of *n* experiments/samples. Significant differences were determined using R software (www.R-project.org) or Student's *t*-test. Significance was set at $p < .05$.

RESULTS

Surface Area and Size Distribution of TiO_2 Particles

To measure the surface area and size distribution of TiO_2 particles, a Gemini 2360 surface area analyzer and scanning electron microscopy were used, respectively. The average surface area of TiO_2 nanoparticles was 49.00 m^2/g, compared to 2.28 m^2/g for fine particles. The surface area of TiO_2 nanoparticles is 21-fold greater than TiO_2 fine particles. The average size distribution of TiO_2 nanoparticles or fine particles was 34.90 nm and 1.22 μm, respectively (Table 1).

TABLE 1
Surface Area and Size Distribution of TiO_2 Particles

	TiO_2 fine particles	TiO_2 nano particles
Surface area (m^2/g)	2.28 ± 0.07	49.0 ± 0.38
Average size	1.22 ± 0.33 (μm)	34.9 ± 16.80 (nm)

Note. Surface area was determined by gas absorption and particle size by scanning electron microscopy. Values are means ± SE of six independent assays.

Effects of TiO_2 Particles on Cell Viability

To determine whether there was a difference in the cytotoxicity induced by TiO_2 nanoparticles or fine particles, serial concentrations of both particles from 0.1 to 20 μg/cm^2 were used to study their effects on cell viability in JB6 cells using the MTT assay. Treatment of JB6 cells with TiO_2 particles for 24 h produced a concentration-dependent cytotoxicity (Figure 1A). Significantly higher cytotoxicity was observed in cells treated with TiO_2 nanoparticles when compared to fine particles using same mass concentrations.

Apoptosis Induced by TiO_2 Particles

To study the induction of apoptosis by TiO_2 nanoparticles or fine particles, YP staining was used. Results indicate that both TiO_2 nanoparticles and fine particles induced apoptosis in a concentration-dependent manner (Figure 1B). The induction of apoptosis was significantly higher after cells were exposed to nanoparticles compared to fine particles (Figure 1C). At concentrations of 5 and 10 μg/cm^2, the apoptotic cell numbers induced by nanoparticles were two- and threefold higher, respectively, than fine particles.

Distinguishing Between Apoptosis and Necrosis Induced by TiO_2 Nanoparticles

A dual staining assay using YP and PI was applied to distinguish between apoptosis and necrosis. YP, a green fluorescent dye, enters cells once their plasma membrane has reached a

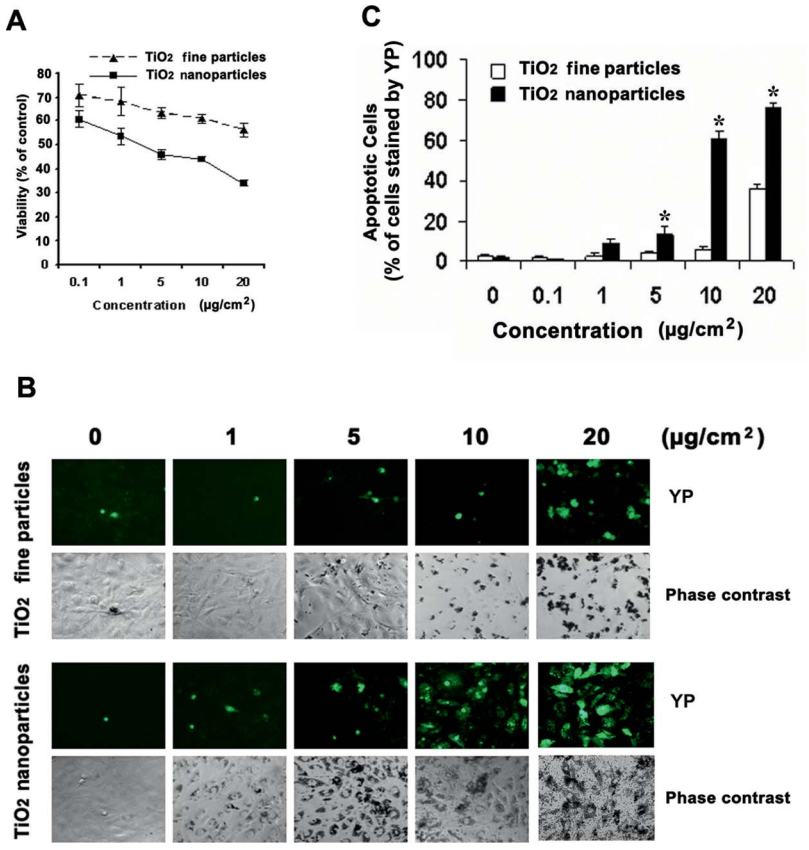

FIG. 1. Effects of TiO_2 particles on cell viability and apoptotic induction. (A) JB6 cells were exposed to various concentrations of TiO_2 nanoparticles or fine particles for 24 h. Cell viability was detected by the MTT assay. Data shown are means ± SE of four independent assays. (B) Apoptosis was detected by YP staining. Both TiO_2 nanoparticles and fineparticles induced JB6 cell apoptosis (10 × magnification). (C) Data shown are means ± SE of three independent assays. Asterisk indicates significant difference from fine particles ($p < .05$).

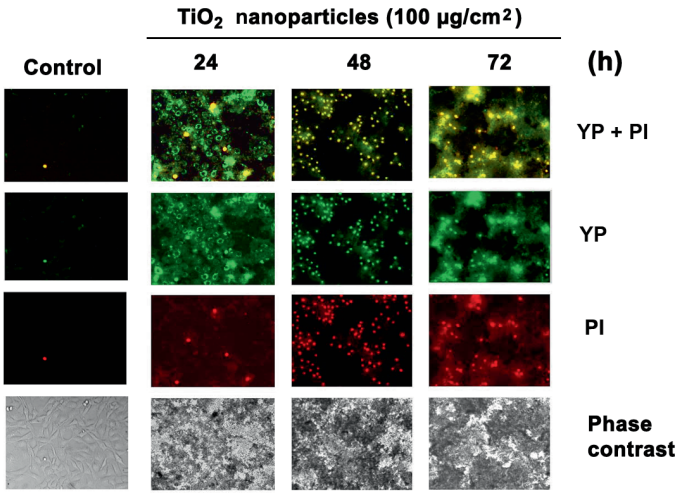

FIG. 2. Distinguishing between apoptosis or necrosis induced by TiO_2 nanoparticles. Cells were treated with/without TiO_2 nanoparticles. Continuous monitoring of apoptosis and necrosis was conducted by using a dual fluorescence dye assay at different incubation time points (10 × magnification).

certain degree of permeability in apoptotic cells (Idziorek et al., 1995; Liu et al., 2004). PI, a red fluorescent dye, is applied to stain for necrosis with its red fluorescence. The intact cell membrane of viable cells is impermeable to both YP and PI dyes. The results show that TiO_2 nanoparticles induced apoptosis in JB6 cells (stained by YP only) at early exposure time 24 h. However, after prolonged treatment (48–72 h), cells were necrotic (stained by both YP and PI; Figure 2).

Effects of TiO_2 Particles on Caspase-8, Bid, BAX, Bcl-2, Caspase-3, and PARP

Previous studies demonstrated that apoptosis requires activation of an upstream protease caspase-8 (Ashkenazi & Dixit, 1999; Robison et al., 1982). To determine whether TiO_2 particles induce the activation of this caspase, JB6 cells were treated with 100 µg/cm^2 TiO_2 nanoparticles or fine particles for 30, 60, 120, or 180 min, and protease activity was examined by Western-blot analysis. The results indicated that both TiO_2 nanoparticles and TiO_2 fine particles activated caspase-8 in JB6 cells. The TiO_2 nanoparticles elicited more potent caspase-8 activation than TiO_2 fine particles (Figure 3A).

Bid, a proapoptotic member of the Bcl-2 family, is a physiological substrate of caspase-8 that is responsible for mitochondrial damage (Belka et al., 2000; Luo et al., 1998). Whether activation of caspase-8 induced by TiO_2 particles was followed by the proteolytic activation of Bid was determined. Expression alterations of other Bcl-2 family members were also investigated. Western blot analysis demonstrated that TiO_2 particles induced Bid cleavage in JB6 cells. BAX, a proapoptotic member of the Bcl-2 family, was also activated, while anti-apoptotic protein Bcl-2 was downregulated. In general, TiO_2 nanoparticles appeared to be more potent than fine particles in their effect on the Bcl-2 family members (Figure 3B).

Caspase-3 is critical in executing apoptosis, as it is either partially or totally responsible for the proteolytic cleavage of many key proteins. The effect of TiO_2 particles on the activation of caspase-3 was investigated. TiO_2 nanoparticles induced activation of caspase-3 as shown by cleavage of caspase-3. TiO_2 fine particles showed a transient activation of caspase-3 (Figure 3C).

The activation of downstream caspase-3 results in activation of PARP (Robison et al., 1982; Tewari et al., 1995). To detect PARP cleavages, cells were treated with TiO_2 particles for 30, 60, 120, or 180 min. PARP cleavages were examined by Western blot analysis. TiO_2 nanoparticles produced significant activation of cleaved PARP at 60 min postexposure and declined at 120 min. TiO_2 fine particles showed a weak activation of cleaved PARP at 180 min postexposure (Figure 3D).

TiO_2 Particles Induce Cytochrome *c* Release from the Mitochondria to Cytosol

Caspase-8-mediated cleavage of Bid leads to release of cytochrome *c* from the mitochondria to cytosol, which is an essential step in the induction of apoptosis (Grossmann et al., 1998; Luo et al., 1998). To determine whether TiO_2 particles induced the release of cytochrome *c* from the mitochondria, the cells were treated with TiO_2 particles for 0.5, 3, 6, or 8 h. Cytochrome *c* release from mitochondria to cytosol was examined by Western-blot analysis. Both TiO_2 nanoparticles and TiO_2 fine particles induced cytochrome *c* release after 6 or 8 h of treatment (Figure 4).

TiO_2 Particles Induce Changes of Mitochondrial Membrane Permeability

Changes in mitochondrial membrane permeability are a hallmark for apoptosis (Charlot et al., 2004; Gadaleta et al., 2005; Piacenza et al., 2007). To determine whether the stability of the mitochondrial membrane was perturbed, JB6 cells were treated with or without various concentrations of TiO_2 nanoparticles. After 24 h of incubation, changes of the mitochondrial membrane permeability were evaluated. The results show that TiO_2 nanoparticles increase mitochondrial membrane permeability in a concentration-dependent manner. Positive control cells treated with 0.5 µl valinomycin/cm^2 for 1 h showed a significant effect on the mitochondrial membrane permeability (Figure 5).

DISCUSSION AND CONCLUSION

TiO_2 nanoparticles are widely used in many industrial applications and consumer products today (Sayes et al., 2006). In this study, both TiO_2 nanoparticles and fine particles induced apoptosis in JB6 cells. TiO_2 nanoparticles elicited higher cytotoxicity and apoptosis induction than fine particles. TiO_2

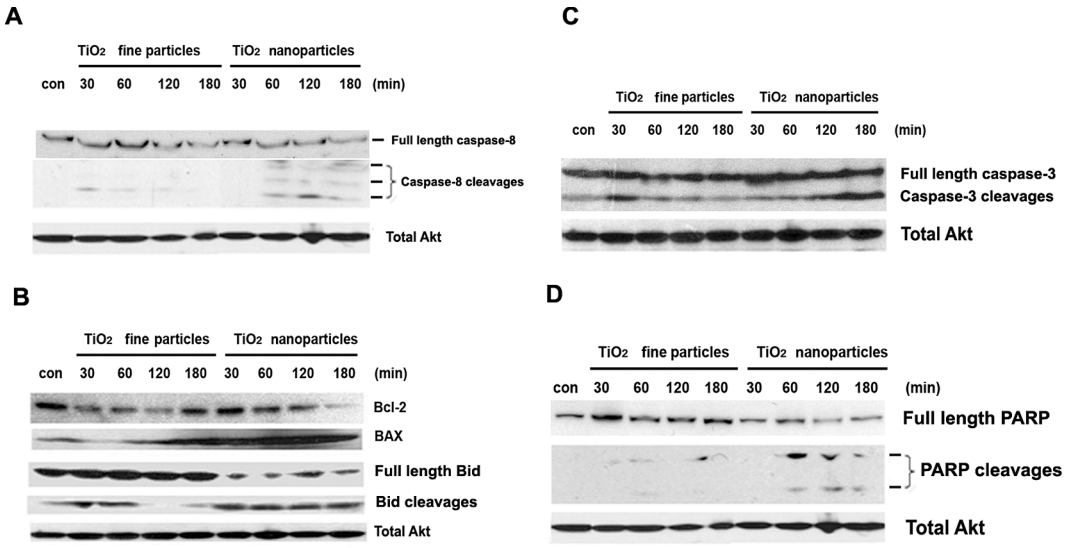

FIG. 3. Effects of TiO_2 particles on caspase-8, Bid, BAX, Bcl-2, caspase-3, and PARP. Cells were seeded onto a six-well plate. After 24 h of incubation, cells were starved in 0.1% FBS EMEM overnight. Western blot was performed after cells were treated with/without TiO_2 nanoparticles or fine particles for different time points.

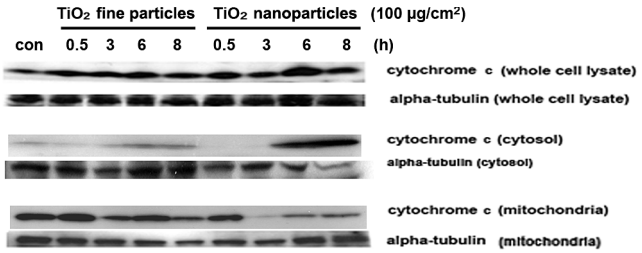

FIG. 4. Effect of TiO_2 particles on cytochrome *c* release. Cells were seeded onto a six-well plate. After 24 h of incubation, cells were starved in 0.1% FBS EMEM overnight. Western blot was performed after cells were treated with/without TiO_2 nanoparticles or fine particles for different time periods.

nanoparticles activated caspase-8, Bid, BAX, caspase-3, and PARP, leading to downregulation of Bcl-2 and increased mitochondrial membrane permeability.

To compare the cytotoxicity induced by TiO_2 particles, two different sizes of TiO_2 particles, namely, nanoparticles and fine particles, were used in this study. TiO_2 nanoparticles were an 80/20% mixture of the anatase and rutile forms of TiO_2, with an average size of 21 nm. TiO_2 fine particles were a predominantly rutile form particle with an average diameter less than 5 μm. MTT assay results showed that both TiO_2 nanoparticles and fine particles induced cytotoxicity in JB6 cells after 24 h of exposure in a concentration-dependent manner. Fine-sized TiO_2 particles are commonly regarded as a low-toxicity dust that is considered to be virtually inert (Bermudez et al., 2002). It has been widely used as a negative control in inhalation and toxicity studies (Warheit et al., 1997). The present study indicates that TiO_2 nanoparticles produced significantly higher cytotoxicity than fine particles. Our findings are in agreement with previous *in vivo* reports that TiO_2 nanoparticles are more toxic than fine particles (Driscoll et al., 1990; Oberdorster et al., 1994). To our knowledge, the present study provides the first evidence that both TiO_2 nanoparticles and TiO_2 fine particles, although the latter previously considered a biologically inert, elicit cytotoxicity in JB6 cells *in vitro*.

Cell death may occur by either of two distinct mechanisms, apoptosis or necrosis. Apoptotic cells are characterized by a number of morphologic, molecular, and biochemical features (Darzynkiewicz et al., 1992; Kerr et al., 1972). Necrosis produces a leakage of cell content. A study (Rahman et al., 2002) found TiO_2 nanoparticles induced typical appearance of characteristic changes for apoptosis in SHE cells. For the quantification of apoptosis, YP staining was carried out to determine apoptosis induced by various concentrations of TiO_2 nanoparticles or TiO_2 fine particles. Our results indicated that TiO_2 nanoparticles induced greater apoptosis than TiO_2 fine particles. To distinguish apoptosis from necrosis induced by TiO_2 nanoparticles, YP/PI dual staining (Gawlitta et al., 2004) was used in the present study. Our results indicated that TiO_2 nanoparticles induced cell apoptosis but not necrosis at early exposure times (24 h). With prolonged treatment (48–72 h), TiO_2 nanoparticles induced JB6 cells necrosis. In a 3-mo inhalation study in rats, Oberdorster et al. (1994) found nanoscale TiO_2 to be more inflammatory than fine-sized TiO_2. When results were normalized to surface area, the authors found that the concentration-response curves for nanoparticles and fine-sized TiO_2-particles were similar, suggesting that the pulmonary inflammation was mediated by surface effects. Our results indicate that both TiO_2 nanoparticles and TiO_2 fine particles

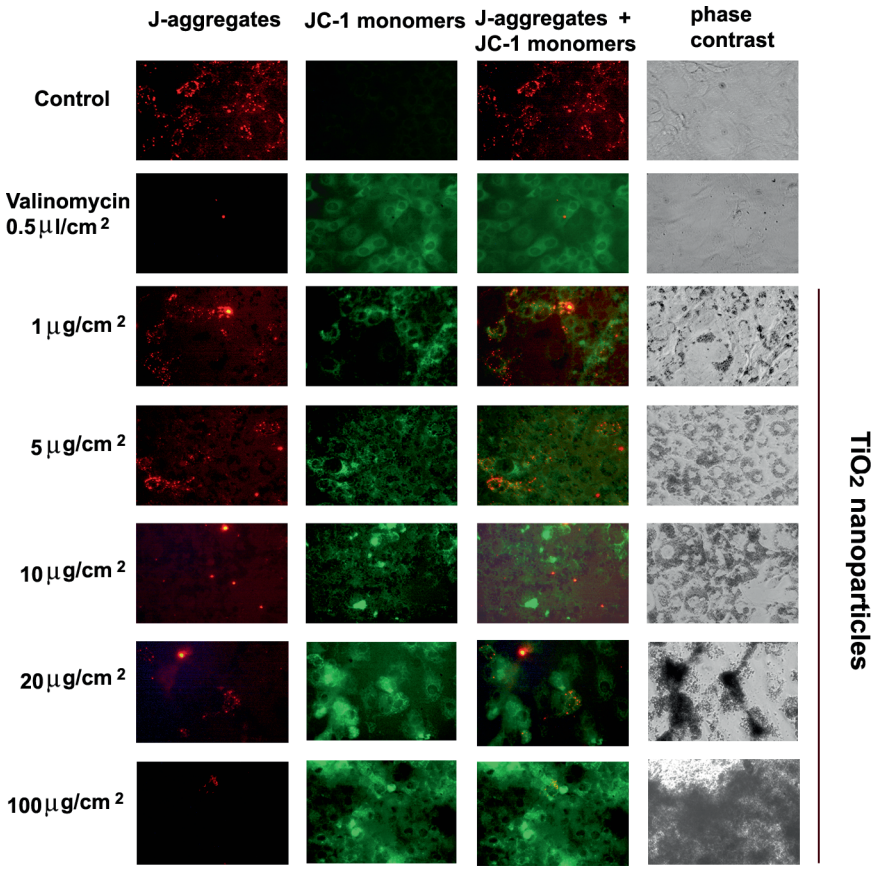

FIG. 5. Effect of TiO_2 nanoparticles on mitochondrial membrane permeability**.** JB6 cells were treated with TiO_2 nanoparticles for 24 h. A mitochondrial staining kit was used to detect the mitochondrial membrane permeability (20 × magnification).

are toxic and induce apoptosis in JB6 cells, while TiO_2 nanoparticles show higher cytotoxicity and apoptosis induction than TiO_2 fine particles. By gas absorption, the surface area of TiO_2 nanoparticles is 21-fold greater than that of TiO_2 fine particles. However, TiO_2 nanoparticles exhibited potency for toxicity and apoptosis that was somewhat less than 21-fold greater than fine particles. Therefore, surface area tends to overcorrect for the greater toxicity.

In this study, signal pathways involved in TiO_2 nanoparticle-induced apoptosis were investigated. Caspases play a critical role in regulating many of the morphological and biochemical features of apoptosis. The role of caspase-8 in the triggering of apoptosis was demonstrated as an apical initiator caspases in receptor- and stress-induced apoptosis (Lombaert et al., 2004). In death receptor-initiated apoptosis, the activation of the initiator procaspase-8 is the decision point for further signaling toward apoptosis (Lombaert et al., 2004). Our results show that TiO_2 particles activate caspase-8, which is associated with cleavage of Bid. Cleavage of Bid was reported to translocate from the cytoplasm to the mitochondria and induce cytochrome *c* release (Grossmann et al., 1998). The Bcl-2 proteins are a family of proteins involved in the response to apoptosis. Some of these proteins, such as Bcl-2, are anti-apoptotic, while others (such as BAX, Bid, or Bad) are pro-apoptotic. The Bcl-2 family of proteins controls mitochondrial integrity, whereby the balance of pro-apoptotic BAX and anti-apoptotic Bcl-2 protein determines the relative sensitivity of cells to apoptotic stimuli (Oltvai & Korsmeyer, 1994). Our data show that both TiO_2 nanoparticles and TiO_2 fine particles induce activation of the pro-apoptotic protein BAX and downregulation of anti-apoptotic protein Bcl-2. An excess of BAX and a decrease of Bcl-2 at the surface of the mitochondria may be important in the formation of the permeability transition pore and in the release of cytochrome *c*. Cytochrome *c* release from mitochondria to cytosol in turn leads to the activation of the caspase cascade such as caspase-3. The activation of caspase-3 produces cleavage of PARP. These results suggest that TiO_2 particles induce apoptosis in JB6 cells through activation of caspase-8/Bid and mitochondrial pathways.

Mitochondria play an important role in the regulation of cell death. Any change in the mitochondrial membrane permeability is known to be an early event in apoptosis. Many pro-apoptotic proteins are released from the mitochondria into the cytosol, following the formation of a permeability transition pore in the

mitochondrial membrane. To elucidate the involvement of mitochondria in the process of apoptosis induced by TiO_2 nanoparticles, changes of the mitochondrial membrane permeability were evaluated using a mitochondrial staining kit. Our data show that using dye JC-1 (5,5′,6,6'-tetrachloro-1,1′,3,3′-tetraethylbenzimidazolocarbocyanine iodide) is a fast and convenient method for detection of the changes in mitochondrial membrane permeability in living cells. In normal cells, due to the electrochemical potential gradient, the dye JC-1 concentrates in the mitochondrial matrix where it forms red fluorescent aggregates (J-aggregates). Any event that dissipates the mitochondrial membrane potential prevents the accumulation of the JC-1 dye in the mitochondria, and thus the dye is dispersed throughout the entire cell, leading to a shift from red (J-aggregates) to green fluorescence (JC-1 monomers). In this study, TiO_2 nanoparticles increased mitochondrial membrane permeability in a concentration-dependent manner, which is in agreement with the release of cytochrome *c* from mitochondria to cytosol detected by Western blot analysis. These findings imply the involvement of mitochondria in the process of apoptosis induced by TiO_2 nanoparticles in JB6 cells.

In summary, the major findings of the present study include: (1) TiO_2 nanoparticles induce JB6 cell apoptosis through activation of caspase-8/Bid pathway; (2) mitochondrial membrane permeability injury may be involved in the process of apoptosis induced by TiO_2 nanoparticles; and (3) TiO_2 nanoparticles elicit higher cytotoxicity and apoptotic induction than fine particles in JB6 cells.

REFERENCES

Ashkenazi, A., and Dixit, V. M. 1999. Apoptosis control by death and decoy receptors. *Curr. Opin. Cell. Biol*. 11:255–260.

Baggs, R. B., Ferin, J., and Oberdorster, G. 1997. Regression of pulmonary lesions produced by inhaled titanium dioxide in rats. *Vet. Pathol*. 34: 592–597.

Bardales, R. H., Xie, S. S., Schaefer, R. F., and Hsu, S. M. 1996. Apoptosis is a major pathway responsible for the resolution of type II pneumocytes in acute lung injury. *Am. J. Pathol*. 149: 845–852.

Belka, C., Rudner, J., Wesselborg, S., Stepczynska, A., Marini, P., Lepple-Wienhues, A., Faltin, H., Bamberg, M., Budach, W., and Schulze-Osthoff, K. 2000. Differential role of caspase-8 and BID activation during radiation- and CD95-induced apoptosis. *Oncogene*. 19:1181–1190.

Bermudez, E., Mangum, J. B., Asgharian, B., Wong, B.A., Reverdy, E. E., Janszen, D. B., Hext, P. M., Warheit, D. B., and Everitt, J. I. 2002. Long-term pulmonary responses of three laboratory rodent species to subchronic inhalation of pigmentary titanium dioxide particles. *Toxicol Sci*. 70:86–97.

Boffa, D. J., Waka, J., Thomas, D., Suh, S., Curran, K., Sharma, V. K., Besada, M., Muthukumar, T., Yang, H., Suthanthiran, M., and Manova, K. 2005. Measurement of apoptosis of intact human islets by confocal optical sectioning and stereologic analysis of YO-PRO-1-stained islets. *Transplantation* 79:842–845.

Charlot, J. F., Pretet, J. L., Haughey, C., and Mougin, C. 2004. Mitochondrial translocation of p53 and mitochondrial membrane potential (Delta Psi m) dissipation are early events in staurosporine-induced apoptosis of wild type and mutated p53 epithelial cells. *Apoptosis* 9:333–343.

Churg, A., Gilks, B., and Dai, J. 1999. Induction of fibrogenic mediators by fine and ultrafine titanium dioxide in rat tracheal explants. *Am. J. Physiol*. 277:L975–L982.

Churg, A., Stevens, B., and Wright, J. L. 1998. Comparison of the uptake of fine and ultrafine TiO_2 in a tracheal explant system. *Am. J. Physiol*. 274:L81–L86.

Darzynkiewicz, Z., Bruno, S., Del Bino, G., Gorczyca, W., Hotz, M. A., Lassota, P., and Traganos, F. 1992. Features of apoptotic cells measured by flow cytometry. *Cytometry* 13:795–808.

Driscoll, K. E., Maurer, J. K., Lindenschmidt, R.C., Romberger, D., Rennard, S. I., and Crosby, L. 1990. Respiratory tract responses to dust: Relationships between dust burden, lung injury, alveolar macrophage fibronectin release, and the development of pulmonary fibrosis. *Toxicol. Appl. Pharmacol*. 106:88–101.

Durmowicz, A. G., and Stenmark, K. R. 1999. Mechanisms of structural remodeling in chronic pulmonary hypertension. *Pediatr. Rev*. 20:e91–e102.

Gadaleta, P., Perfetti, X., Mersich, S., and Coulombie, F. 2005. Early activation of the mitochondrial apoptotic pathway in vesicular stomatitis virus-infected cells. *Virus Res*. 109:65–69.

Gawlitta, D., Cees, W. J., Oomens, F. P., Baaijens, P. T., and Bouten, C. V. C. 2004. Evaluation of a continuous quantification method of apoptosis and necrosis in tissue cultures. *Cytotechnology* 46:139–150.

Grossmann, J., Mohr, S., Lapentina, E. G., Fiocchi, C., and Levine, A. D. 1998. Sequential and rapid activation of select caspases during apoptosis of normal intestinal epithelial cells. *Am J Physiol*. 274:G1117–G1124.

IARC. 2006. Cobalt in hard metals and cobalt sulfate, gallium arsenide, indium phosphide and vanadium pentoxide. *IARC Monogr. Eval. Carcinogen. Risks Hum*. 86.

Idziorek, T., Estaquier, J., De Bels, F., and Ameisen, J. C. 1995. YOPRO-1 permits cytofluorometric analysis of programmed cell death (apoptosis) without interfering with cell viability. *J. Immunol. Methods* 185:249–258.

Kaida, T., Kobayashi, K., Adachi, M., and Suzuki, F. 2004. Optical characteristics of titanium oxide interference film and the film laminated with oxides and their applications for cosmetics. *J. Cosmet. Sci*. 55:219–220.

Kerr, J. F., Wyllie, A. H., and Currie, A. R. 1972. Apoptosis: A basic biological phenomenon with wide-ranging implications in tissue kinetics. *Br. J. Cancer* 26:239–257.

Kuwano, K., Miyazaki, H., Hagimoto, N., Kawasaki, M., Fujita, M., Kunitake, R., Kaneko, Y., and Hara, N. 1999. The involvement of Fas–Fas ligand pathway in fibrosing lung diseases. *Am. J. Respir. Cell Mol. Biol*. 20:53–60.

Lademann, J., Weigmann, H., Rickmeyer, C., Barthelmes, H., Schaefer, H., Mueller, G., and Sterry, W. 1999. Penetration of titanium dioxide microparticles in a sunscreen formulation into the horny layer and the follicular orifice. *Skin Pharmacol. Appl. Skin Physiol*. 12:247–256.

Lee, K. P., Trochimowicz, H. J., and Reinhardt, C. F. 1985. Pulmonary response of rats exposed to titanium dioxide (TiO_2) by inhalation for two years. *Toxicol. Appl. Pharmacol*. 79:179–192.

Levine, A. J. 1997. p53, the cellular gatekeeper for growth and division. *Cell* 88:323–331.

Liu, X., Van Vleet, T., and Schnellmann, R. G. 2004. The role of calpain in oncotic cell death. *Annu. Rev. Pharmacol. Toxicol*. 44:349–370.

Lombaert, N., De Boeck, M., Decordier, I., Cundari, E., Lison, D., and Kirsch-Volders, M. 2004. Evaluation of the apoptogenic potential of hard metal dust (WC-Co), tungsten carbide and metallic cobalt. *Toxicol. Lett*. 154:23–34.

Long, T. C., Tajuba, J., Sama, P., Saleh, N., Swartz, C., Parker, J., Hester, S., Lowry, G. V., and Veronesi, B. 2007. Nanosize titanium dioxide stimulates reactive oxygen species in brain microglia and damages neurons in vitro. *Environ. Health Perspect*. 115:1631–1637.

Luo, X., Budihardjo, I., Zou, H., Slaughter, C., and Wang, X. 1998. Bid, a Bcl2 interacting protein, mediates cytochrome c release from mitochondria in response to activation of cell surface death receptors. *Cell* 94:481–490.

Luther, W. E. 2004. Industrial application of nanomaterials—Chances and risks. *Future Technol*. 54:1–112.

Matute-Bello, G., Winn, R. K., Jonas, M., Chi, E. Y., Martin, T. R., and Liles, W. C. 2001. Fas (CD95) induces alveolar epithelial cell apoptosis in vivo: Implications for acute pulmonary inflammation. *Am. J. Pathol*. 158:153–161.

Oberdorster, G., Ferin, J., and Lehnert, B. E. 1994. Correlation between particle size, in vivo particle persistence, and lung injury. *Environ. Health Perspect.* 102(suppl. 5):173–179.

Oltvai, Z. N., and Korsmeyer, S. J. 1994. Checkpoints of dueling dimers foil death wishes. *Cell* 79:189–192.

Piacenza, L., Irigoin, F., Alvarez, M. N., Peluffo, G., Taylor, M. C., Kelly, J. M., Wilkinson, S. R., and Radi, R. 2007. Mitochondrial superoxide radicals mediate programmed cell death in *Trypanosoma cruzi*: Cytoprotective action of mitochondrial iron superoxide dismutase overexpression. *Biochem. J*. 403:323–334.

Raff, M. C. 1992. Social controls on cell survival and cell death. *Nature* 356:397–400.

Rahman, Q., Lohani, M., Dopp, E., Pemsel, H., Jonas, L., Weiss, D. G., and Schiffmann, D. 2002. Evidence that ultrafine titanium dioxide induces micronuclei and apoptosis in Syrian hamster embryo fibroblasts. *Environ. Health Perspect.* 110:797–800.

Robison, S. H., Cantoni, O., and Costa, M. 1982. Strand breakage and decreased molecular weight of DNA induced by specific metal compounds. *Carcinogenesis* 3:657–662.

Sayes, C. M., Wahi, R., Kurian, P. A., Liu, Y., West, J. L., Ausman, K. D., Warheit, D. B., and Colvin, V. L. 2006. Correlating nanoscale titania structure with toxicity: A cytotoxicity and inflammatory response study with human dermal fibroblasts and human lung epithelial cells. *Toxicol. Sci*. 92:174–185.

Steller, H. 1995. Mechanisms and genes of cellular suicide. *Science* 267: 1445–1449.

Tabet, L., Bussy, C., Amara, N., Setyan, A., Grodet, A., Rossi, M. J., Pairon, J. C., Boczkowski, J., and Lanone, S. 2009. Adverse effects of industrial multiwalled carbon nanotubes on human pulmonary cells. *J. Toxicol. Environ. Health A* 72:60–73.

Tewari, M., Quan, L. T., O'Rourke, K., Desnoyers, S., Zeng, Z., Beidler, D. R., Poirier, G. G., Salvesen, G. S., and Dixit, V. M. 1995. Yama/CPP32 beta, a mammalian homolog of CED-3, is a CrmA-inhibitable protease that cleaves the death substrate poly(ADP-ribose) polymerase. *Cell* 81:801–809.

Wang, J. J., Sanderson, B. J., and Wang, H. 2007. Cyto- and genotoxicity of ultrafine TiO2 particles in cultured human lymphoblastoid cells. *Mutat Res*. 628:99–106.

Warheit, D. B., Hansen, J. F., Yuen, I. S., Kelly, D. P., Snajdr, S. I., and Hartsky, M. A. 1997. Inhalation of high concentrations of low toxicity dusts in rats results in impaired pulmonary clearance mechanisms and persistent inflammation. *Toxicol. Appl. Pharmacol*. 145:10–22.

White, S. R., Williams, P., Wojcik, K. R., Sun, S., Hiemstra, P. S., Rabe, K. F., and Dorscheid, D. R. 2001. Initiation of apoptosis by actin cytoskeletal derangement in human airway epithelial cells. *Am. J. Respir. Cell Mol. Biol*. 24:282–294.

Wolf, R., Matz, H., Orion, E., and Lipozencic, J. 2003. Sunscreens—The ultimate cosmetic. *Acta Dermatovenerol. Croat*. 11:158–162.

Wyllie, A. H., Kerr, J. F., and Currie, A. R. 1980 Cell death: The significance of apoptosis. *Int. Rev. Cytol*. 68:251–306.